©2022 Published in 10th International Symposium on Innovative Technologies in Engineering and Science 21-23 October 2022 (ISITES2022 Bursa - Turkey)
https://doi.org/10.33793/acperpro.05.03.7422

Edge Detection Based Autofocus Algorithm to Detect Accurate Camera Working Distance

[1,2]Mehmet Kacmaz and [1,2*]Ahmet Gokhan Poyraz
[1*] Dogu Pres R&D Center, 16140 Bursa/Turkey
[2] Bursa Technical University – Electrical and Electronics Engineering, 16310, Bursa, Turkey

Abstract

In the last 10 years, industrial image processing has been used in many areas such as automotive, medicine and aviation. Especially for sensitive measurement applications, camera control systems are preferred due to their speed and quality advantages. In this study, a method is proposed to determine the optimum camera position at the image acquisition phase for industrial cameras. In the proposed approach, images are captured while the camera and telecentric lens, which are connected to the servo motor, are moving up and down. The edge informations of the captured images are extracted in the x and y directions and the amplitude value is calculated. Then, meaningful and meaningless edge information at each motor position is found with a median-based approach. Finally, the sharpness of the images are arranged by statistical analysis and the optimum focal point for the camera is found. Sobel, Robert and Prewitt Filters were applied to determine the best method for extracting edge information. Measurements were performed on the workpieces using camera positions where the focus was optimum for each method. According to the results, it has been observed that the camera position, which produces the closest result to the real values, is obtained from the focus determined by the Sobel Filter. The proposed method is leaded to researchers to provide automatic focus for camera control systems.

Key words: Industrial Image Processing, Autofocus, Sobel, Camera, Measurement

1. Introduction

Camera technologies are used in a wide range from daily life to industrial production areas. One of the most important stages in the developing manufacturing industry is the post-production quality-control process. Since it is very difficult and troublesome to pass the quality-control process one by one for industrial parts with a very high production amount, a system with the ability to perform serial control operations is needed. At this point, the quality control process can be accelerated by using industrial cameras and image processing algorithms. However, the narrow focal distance range, which is one of the biggest problems of industrial cameras, causes serious errors in size measurements on parts with sensitive tolerance ranges. The distance between the part to be imaged and the lens should be at the optimum distance. When the camera focus is adjusted manually, the sensitivity may not reach the desired position. This situation causes variability in measurement results and measurement success. Therefore, healthier measurements will be obtained by finding the optimum image distance between camera lens and the surface of the part.

In focus applications, the determination of the position where the focus point is best can be done in two basic ways. The first is active AF, where focusing is achieved with ultrasonic or IR sensors integrated into the camera. The reflection of the wave or beam sent through the sensors on the

*Corresponding author: Ahmet Gökhan POYRAZ, Address: Dogu Pres R&D Center, E-mail address: agpoyraz@gmail.com, gokhanpoyraz@dogupres.com, Phone: + (0224) 219 00 50

camera is waited. Then, when the reflected signal is received, the distance of the imaged object can be found by using the velocity-time relationship. If a lens is to be used, the sensors can also be adjusted at lens level. Active AF is already common in DSC (Digital Still Camera) technologies. However, active AF comes with cost and high power consumption. The second approach, passive AF, is based entirely on the quality of the captured image, without using any extra components. In the passive approach, it is also important what kind of images the focusing process will be made on. A focusing algorithm for dimension measurement in industrial parts may not give the same performance in everyday photographs. In this approach, the same part is viewed repeatedly at different distances, and the sharpest image is chosen among the obtained images. The sharpness detection methods used in the literature are obtained as a result of operations in the spatial and frequency domains. Spatial methods are generally obtained by performing operations on edge information. Passive focusing methods are shown and compared in Ref [1]. The method, which is shown as the best among these methods, is the Tenegrade measurement, is created through thresholding the gradient magnitude. Nayar [2] developed a more robust method using the Sum-Modified Laplacien (SML) operator. Considering that the focusing quality affects the edge information, the best focus point can be obtained from the image with the sharpest edge information. Some statistical approaches in the literature use edge information as a criterion for sharpness, as in this article [3]. Methods in the frequency domain, on the other hand, obtain the sharpness information by using the high frequency components of the image. Methods such as FFT, DCT, DWT that can be performed in the frequency domain are also used in autofocus applications. The biggest advantage of spatial methods over frequency methods is that they have less processing cost and complexity. In addition, not only these methods, but also neural network-based algorithms have been developed and presented as an alternative to active components [4].

In this study, it is aimed to determine the optimum focal point using industrial cameras. In addition, having less processing cost than other focusing applications is one of the goals to be achieved in this study. The experimental setup consists of a telecentric lens, an industrial camera and a servo motor that can position the camera and lens in the y plane. At fixed intervals, the camera and lens position are moved in a certain direction and images are captured for each position. In the images captured from the camera, the edge values are extracted in the x-y axis. Then, the magnitude values calculated and the edge information of the image at each position obtained with the median-based approach. As a result of statistical analysis, the image with the sharpest edge information is determined among the images captured. The experimental setup positions the camera and lens to the optimum point. In the study, Robert, Prewitt and Sobel filters were used and compared. Images of an industrial part with circular geometry were captured at different camera and lens positions in the experimental setup. Dimension measurements in each image were obtained by Circle Fit algorithm, which will be discussed later. Then, the filter type that gives the closest result to the real values has been determined.

2. Materials and Method

2.1. Experimental Setup

The experimental setup consists of an industrial camera and telecentric lenses placed to measure the radius of the circular metal part placed on the glass surface. As seen in Figure 1(b) the industrial

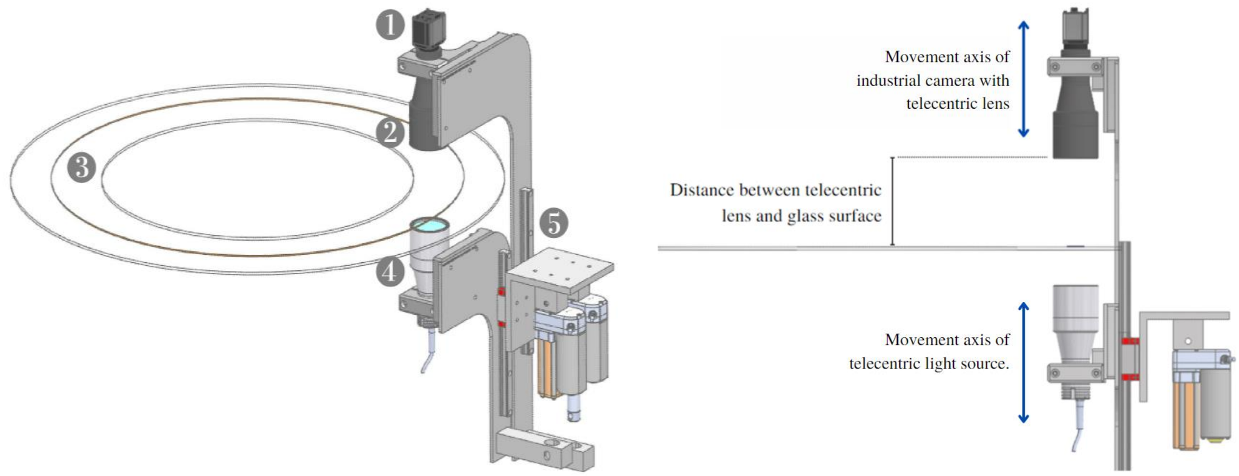

(a) Experimental Setup (b) Experimental Setup Movement System

Figure 1. Experimental Setup Design

has the ability to move in the +y axis, and the telecentric lighting source has the ability to move in the -y axis. This experimental setup created as an image processing based industrial camera control system.

Industrial cameras are the most preferred equipment for control and measurements in mass production areas, thanks to their advantages such as frames per second and high resolution. Telecentric lenses that can be attached to the camera are in an important position for precise measurement. Telecentric lenses have competent advantages such as reflecting light evenly, increased depth of field, equal detector illumination [5]. Telecentric lighting is placed directly opposite the camera's field of view. Camera and telecentric light sources are connected to the experimental setup with servo motors. In this way, the hardware part required for focusing is provided.

Looking at Figure 1, the numbers on the image represent the industrial camera, telecentric lens, rotating glass surface, telecentric light source, and the servo motor that moves the camera & light source components in the y-axis, respectively.

2.2. Industrial Camera and Telecentric Lens

Industrial cameras are more durable than standard cameras. It is especially preferred for quality-control processes in industrial application areas. However, telecentric lenses attached to the camera are also very important for precise measurements. Due to its ability to eliminate perspective, telecentric lenses are widely used to accurately measure the dimensions of objects of different heights [6]. This is because, unlike standard lenses, it transmits light vertically, as seen in Figure 2. In this way, it has the ability to see objects at two different distances and of the same size as if they were in the same position. But its biggest disadvantage is that the optimal focus point is in a rather narrow range. This causes errors and inaccurate measurements in sensitive applications.

Precise optical components and precise alignment are very important to achieve optimum performance in industrial camera control technologies. Telecentric lighting, which is as important as the camera, works differently from standard lighting. In conventional lighting systems, the light

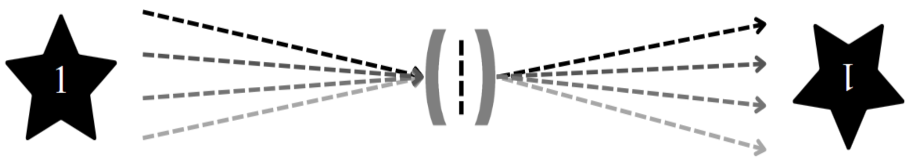

(a) Conventional Lens

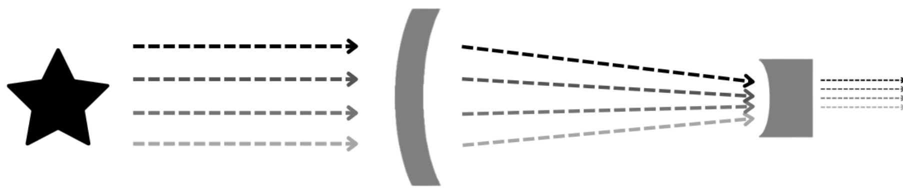

(b) Telecentric Lens

Figure 2. Telecentric Lens – Conventional Lens Comparison

rays expand from the light source and interact with each other, creating a diffuse reflection. In conventional lighting systems, the light rays expand from the light source and interact with each other, creating a diffuse reflection. In telecentric lighting, the light rays leaving the source stay aligned when they hit the surface of an object.

In addition, unlike traditional lighting systems, telecentric illumination has superior features in repeatability and precision measurements. Telecentric illumination does not cause blurry image in edge detection. For these reasons, telecentric illumination was used in the experimental setup. The light source, which must be on the same axis with the camera, also has a certain focusing tolerance range. However, unlike camera lenses, it provides optimum illumination over a wider distance range.

2.3. AF System

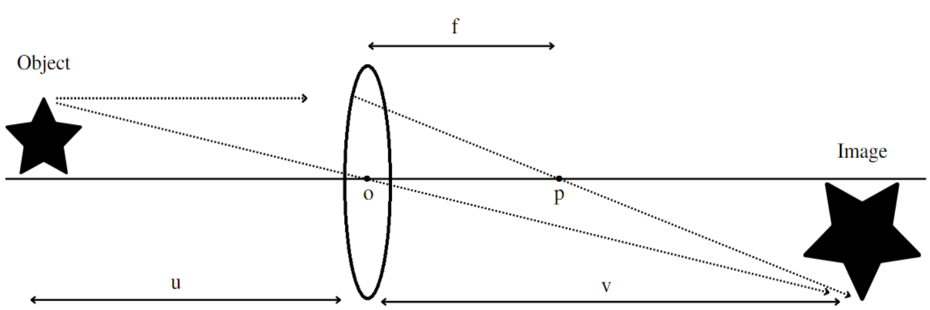

Figure 3. The Focus System Diagram

The focus system is basically given in Figure 3. The working principle can be explained by Eq.1, where f is the focal point, u is the distance between the imaged object and the camera lens.

$$f = \frac{\mathrm{u.v}}{u + v} \tag{1}$$

As the application areas increase, a uniform focusing type does not become sufficient. Therefore, different AF (auto-focus) approaches are used for different applications [7]. In active AF systems, the focusing distance is determined by IR/ultrasonic sensors or a device that can measure the distance between the lens and the part to be imaged, and transfers this information to the camera system [9]. The camera system then adjusts its focus with this information. Active AF is very common and is used in many camera applications [10]. It is also used in industrial and medical devices [11].

Another alternative way to determine the optimal position to obtain high-quality images is Passive AF [12], which can be achieved through image processing. Problems such as high power consumption are eliminated in Passive AF systems that do not require an external sensor or component. Passive AF systems are based on the sharpness of the captured image. After capturing a set of images taken from different distances, the position of the sharpest image gives the best focus point. Since the method used in this study was Passive AF, an external distance measuring device was not needed.

2.4. Theory and Calculation

The most important parameter in AF applications is the sharpness that can be seen at the edges of the captured part. As can be seen in Figure 4(b), a part of a circular geometry part image where we can see the edge information is framed in red. The frame marked here is shown zoomed in Figure 4(c)(d)(e). If the distance between the part and the camera is closer than the optimum focal distance, the blurred image seen in Figure 4(c) will be obtained. As you can see, the transition is smoother and longer. If the distance between the part and the camera is further than the optimum focal distance, a similar blurred image is obtained, as can be seen in Figure 4(e). However, as in Figure 4(d), the clearest image is obtained when the distance between the camera and the part is optimally adjusted. The transition in the edge regions is narrower, the amount of change between the intensity values is higher. From this point of view, edge information contains critical clues about focusing.

First, images of the object are taken with an industrial camera at ε distance intervals. For each captured image, small objects in the image are eliminated and the gradient of the image is found. In order to find the median value of the image significant, all elements with zero value in the obtained image are assigned as undefined. Then all elements in the array that are smaller than the product of the found median value and ς are assigned zero. Finally, a new value is obtained by summing all the elements in the resulting array. The higher this value, the sharper the image.

An I image of the part is captured with a camera capable of moving in the vertical axis. Small objects on the image that do not belong to the part are deleted from the image. Then the gradient of the image is found using a preferred operator (Sobel, Prewitt etc.). The process of finding the gradient of the I image is shown in Equation 2.

$$|\nabla I| = \left[\frac{\partial I}{\partial x}, \frac{\partial I}{\partial y}\right] \tag{2}$$

The magnitude values of the gradient image are obtained using Equation 3. The reason of finding the magnitude value is to detect the high intensity transition that will occur in the edges of the part. The Magnitude value provides information about whether the part is at the optimum focal distance.

$$M = \sqrt{\left(\frac{\partial I}{\partial x}\right)^2 + \left(\frac{\partial I}{\partial y}\right)^2} \tag{3}$$

Using Eq.4, zero-valued elements are removed from the two-dimensional matrix. Before finding the median value, as seen in Eq.5, the mxn matrix M is converted to the kx1 size $\overline{M}$ array.

$$M = \begin{cases} a_{ij}\,, & a_{ij} \neq 0 \\ [\ ]\,, & a_{ij} = 0 \end{cases} \quad \begin{pmatrix} i = 1,2,\dots,m \\ j = 1,2,\dots,n \end{pmatrix} \tag{4}$$

$$M = \begin{bmatrix} a_{11} & \cdots & a_{1n} \\ \vdots & \ddots & \vdots \\ a_{m1} & \cdots & a_{mn} \end{bmatrix} \rightarrow \overline{M} = [\bar{a}_1, \bar{a}_2, \dots, \bar{a}_k] \tag{5}$$

After this process is completed, the median value of the obtained array is found.

$$\sigma = Mdn(\overline{M}) \tag{6}$$

In order to find statistically meaningful edges, values that do not have edge information and therefore have low gradient values should be removed from the array. These values are undesired values. Therefore, values that are smaller than the product of the median and ς will not be considered.

$$\overline{M}(i) = \begin{cases} a_i\,, & i \geq ς \cdot \sigma \\ 0\,, & i < ς \cdot \sigma \end{cases} \quad (i = 1, 2, \dots, k) \tag{7}$$

$\overline{M}$ is the array containing the meaningful edge values. All elements in this array are summed and the total value that obtained gives information about the sharpness level of the image.

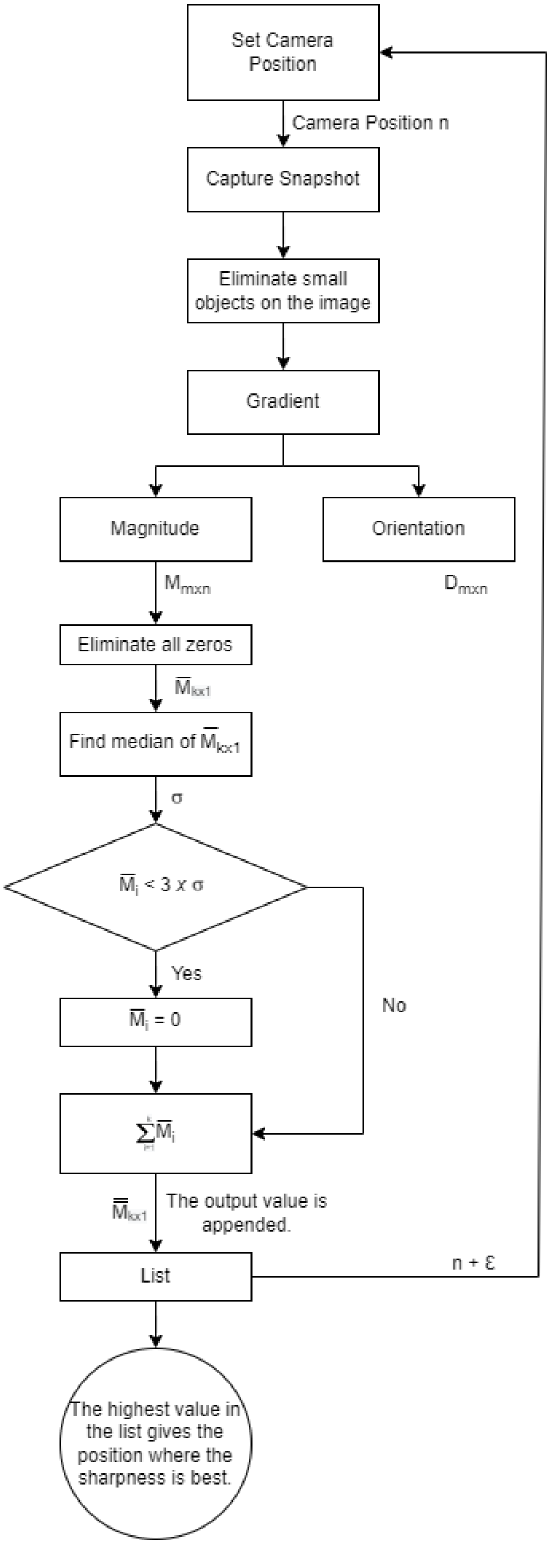

(a) Algorithm Diagram

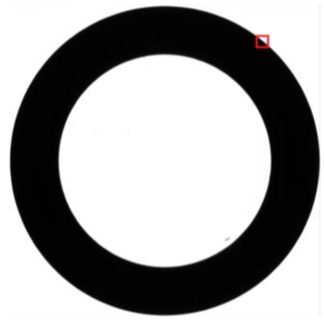

(b) A part with circular geometry captured.

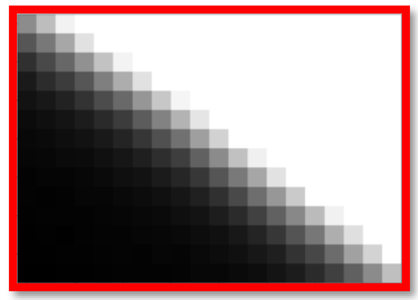

(c) When the camera is behind the optimum focal point

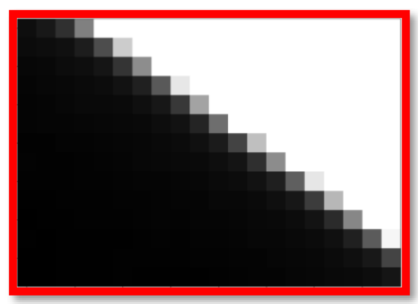

(d) When the camera is at optimum focus.

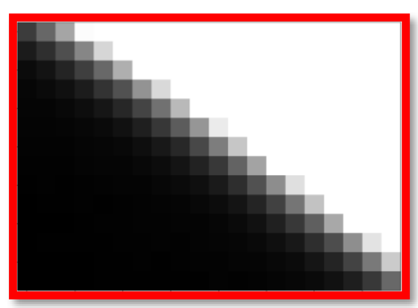

(e) When the camera is ahead of the optimum focal point

Figure 4. Algorithm diagram and the effect of focus on the image.

$$\bar{\bar{M}} = \sum_{i=1}^{k} \bar{M}[i] \tag{8}$$

The resulting value is stored in a list defined as $\bar{\bar{\mathrm{L}}} = \{\bar{\bar{\mathrm{M}}}_1, \bar{\bar{\mathrm{M}}}_2, \ldots, \bar{\bar{\mathrm{M}}}_\mathrm{p}\}$ that contains the obtained value at each distance. When the camera position moves by ε on the vertical axis, all operations are repeated and the new $\bar{\bar{\mathrm{M}}}$ value is added to the $\bar{\bar{\mathrm{L}}}$ list. In this way, different sharpness values are determined at different distances for the camera and the imaged part. The details of the working principle of the median-based AF application can be seen as the algorithm diagram in Figure 4.

Figure 5 shows the working principle of the autofocus approach. After completing the first step in Position 1, an $\bar{\bar{\mathrm{M}}}$value is obtained. Then the same operations are performed in position 2. According to the ε height change value, the operations are repeated at p positions. After the operation is completed at each location, the result values are added to the $\bar{\bar{\mathrm{L}}} = \{\bar{\bar{\mathrm{M}}}_1, \bar{\bar{\mathrm{M}}}_2, \ldots, \bar{\bar{\mathrm{M}}}_\mathrm{p}\}$ list. The position with the highest value in the created list is the height at which the sharpness level is best.

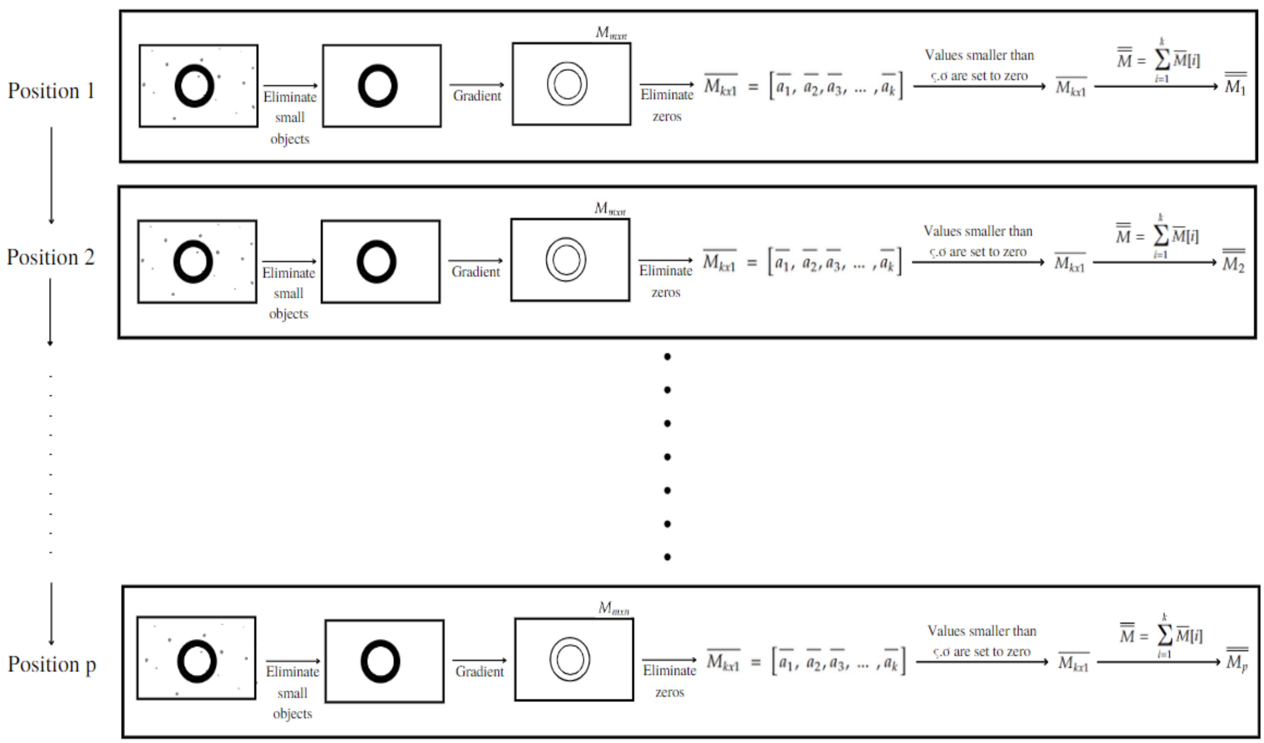

Figure 5. Median Based Auto-Focus Approach Working Principle

3. Results

With this project, a median-based autofocus approach is presented in order to obtain more accurate results in quality-control processes such as surface control and dimensional measurement with industrial camera and lens systems. It has been observed that with this software, which is connected to an automatic system, the position with the best focus can be determined.

In Figure 6(b), the sharpness value-lens position graph for $\varsigma = 10$ is given, and it is the situation where the results closest to the ideal focal point are obtained. The same result was obtained in the size measurements made in Table 2.

Then, ς values were entered as 3, 20, 50, respectively, and deviations were observed after a certain value. The reason for this is, as previously explained; Elements that do not have meaningful edge information and therefore have low gradient values cause errors. As can be seen in Figure 6, as the ς value increases, erroneous values are seen as the focal point. When the ς value is too small, it also causes inaccurate sharpness measurements. As a result of the tests, the use of the variable ς as 10 provides very close results to the reality.

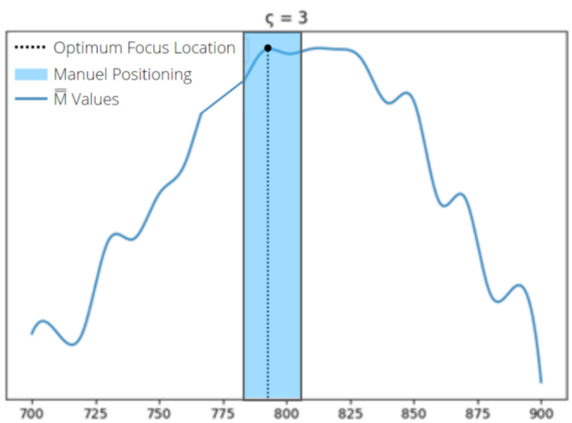

(a) M-Position Graph for $\varsigma = 3$

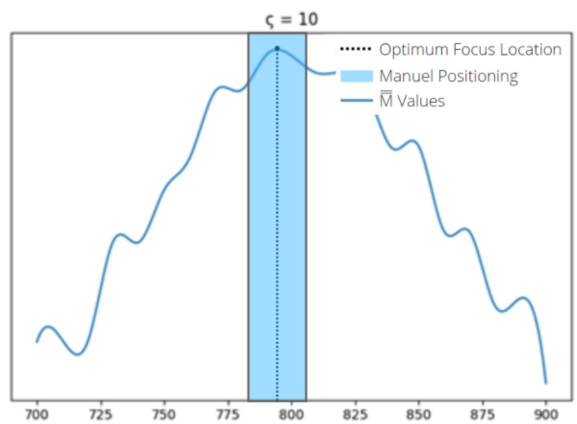

(b) M-Position Graph for $\varsigma = 10$

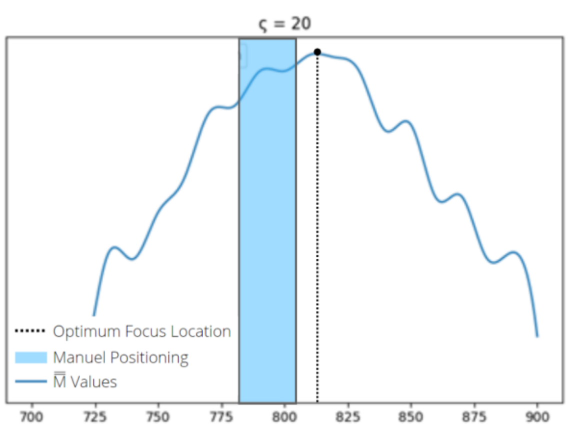

(c) M-Position Graph for $\varsigma = 20$

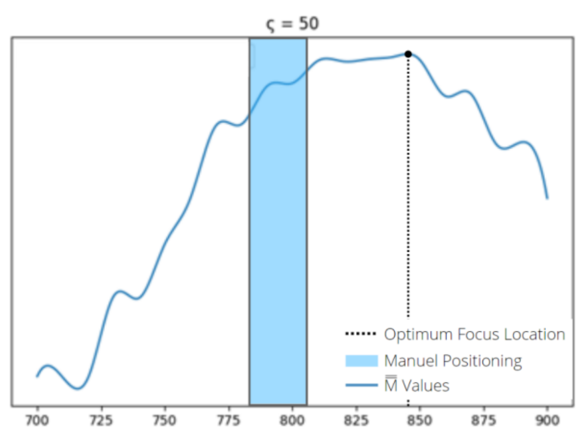

(d) M-Position Graph for $\varsigma = 50$

Figure 6. Sharpness value-position graph for different ς values.

As seen in Table 1, optimum focal distances were obtained for each filter type. Then, in the experimental setup, the camera was moved to the determined location for the filter type to be used. At this stage, which is very important for the next table, images were taken from the optimum positions for each filter.

Table 1. Optimal focus positions with different filters and ς values

Filter Types	Lens Position			
	ς = 3	ς =10	ς = 20	ς = 50
Sobel	**813,04**	**794,31**	**812,37**	**845,15**
Prewitt	812,37	794,31	813,04	845,82
Robert	817,06	825,08	814,38	845,82

Table 2 shows the error percentage between the radius values and the actual values of the part whose images were taken from the focal points obtained by using three different filter types, Sobel, Prewitt and Robert filters. Circle Fit [12] method was used to obtain the radius value. According to obtained values, although the filters obtain results very close to each other. The Sobel operator can detect the sharpest focal point in cases where the ς value is not very high.

Table 2. Percentage of measurement error in images with autofocus adjusted using different filters

Filter Type	Error Rate (%)			
	ς = 3	ς =10	ς = 20	ς = 50
Sobel	**0,81**	**0,03**	**0,63**	1,47
Prewitt	2,06	0,81	1,12	0,91
Robert	1,87	0,67	1,46	**0,49**

Conclusions

In this study, a median-based algorithm for the focusing problem is proposed. The proposed algorithm analyzes the edge information of the images with a median-based approach and finds whether the focus is clear or not. As the experimental setup, a movable camera setup was created. Images were obtained for each position while the camera was moving in the vertical axis. The best focal point is determined by extracting the edge information from the obtained images. First of all, a comparison was made with manual focus. It has been observed that result points of the proposed algorithm is within the manual focusing region. In addition, Sobel, Prewitt and Robert filters are examined for edge detection. In order to test the performance of the filters, the measurements of the known value of the gauge piece at the focal points were examined. According to the results, the Sobel filter gave the least error when ς = 3. The proposed method is aimed to guide the industrial camera control applications.

Appendix

Code: https://github.com/mehmetkacmaz/Median-Based-AutoFocus-Algorithm

4. References

[1] Krotkov, Eric. "Focusing." International Journal of Computer Vision 1.3 (1988): 223-237.
[2] Nayar, Shree K., and Yasuo Nakagawa. "Shape from focus." IEEE Transactions on Pattern analysis and machine intelligence 16.8 (1994): 824-831.
[3] Zhang, Yani, Ying Zhang, and Changyun Wen. "A new focus measure method using moments." Image and Vision computing 18.12 (2000): 959-965.
[4] Chen, Chih-Yung, Rey-Chue Hwang, and Yu-Ju Chen. "A passive auto-focus camera control system." Applied soft computing 10.1 (2010): 296-303.
[5] Li, Dong, and Jindong Tian. "An accurate calibration method for a camera with telecentric lenses." Optics and Lasers in Engineering 51.5 (2013): 538-541.
[6] Pan, Bing, Liping Yu, and Dafang Wu. "High-accuracy 2D digital image correlation measurements using low-cost imaging lenses: implementation of a generalized compensation method." Measurement Science and Technology 25.2 (2013): 025001.
[7] Israni, Dippal, Sandip Patel, and Arpita Shah. "Comparison of different techniques of camera autofocusing." Proceedings of First International Conference on Information and Communication Technology for Intelligent Systems: Volume 1. Springer, Cham, 2016.
[8] Shih, Loren. "Autofocus survey: a comparison of algorithms." Digital photography III. Vol. 6502. SPIE, 2007.
[9] Xu, Xin, et al. "Robust passive autofocus system for mobile phone camera applications." Computers & Electrical Engineering 40.4 (2014): 1353-1362.
[10] Wang, Leyuan, et al. "An End-to-End Autofocus Camera for Iris on the Move." 2021 IEEE International Joint Conference on Biometrics (IJCB). IEEE, 2021.
[11] Fricke, Dierk, et al. "Non-Contact Dermatoscope with Ultra-Bright Light Source and Liquid Lens-Based Autofocus Function." Applied Sciences 9.11 (2019): 2177.
[12] Subbarao, Murali, and JennKwei Tyan. "Optimal focus measure for passive autofocusing and depth-from-focus." Videometrics IV. Vol. 2598. SPIE, 1995.
[13] Bucher, Izhak. "Circle fit." Matlab central file exchange (2004).